LC-PHSM-2001-003
January 10th, 2001

Determination of the $\mathcal{CP}$ quantum numbers of the Higgs boson and test of $\mathcal{CP}$ invariance in the Higgs-strahlung process at a future e^+e^- linear collider.

Markus Schumacher, DESY

Abstract

A complete determination of the profile of the Higgs sector will be one of the central tasks at a future e^+e^- linear collider. The investigation of the $\mathcal{CP}$ properties of the scalar bosons is one important question to be answered. We discuss an analysis exploring the angular distributions of the Z boson in the Higgs-strahlung process. Optimal $\mathcal{CP}$ odd observables are used which allow to test $\mathcal{CP}$ invariance with the highest sensitivity.

1 Introduction

The investigation of the mechanism of electroweak symmetry breaking is one of the central tasks of a future e^+e^- linear collider operating at centre-of-mass energies between 350 and 1000 GeV. If the Higgs mechanism [1] is realized in nature this accelerator will allow to investigate completely and with high accuracy the profile of the Higgs sector. One important part of this is the determination of the $\mathcal{CP}$ quantum numbers of the Higgs bosons, where $\mathcal{C}$ denotes charge conjugation and $\mathcal{P}$ the parity transformation. This might allow to distinguish different models like Standard Model [2](SM), Minimal Supersymmetric Standard Model (MSSM) [3], general Two Higgs Doublet Models (2HDM) and others (see e.g. [4]).

Several methods have been proposed to investigate the $\mathcal{CP}$ properties of the Higgs boson [5]. This analysis considers the Higgs-strahlung process with subsequent decay of the Z boson into a pair of muons. The $\mu^+\mu^-$ H final state allows a clear selection of the signal almost independent of the decay mode of the Higgs boson. The $\mathcal{CP}$ properties of the Higgs boson are extracted from the angular distribution reconstructed from the momenta of the muons.

The analysis reported allows a model independent test of $\mathcal{CP}$ invariance of the Higgs-strahlung process, where the SM does not predict any observable effect of $\mathcal{CP}$ violation. It is instructive to look for new sources of $\mathcal{CP}$ violation beyond the SM, as $\mathcal{CP}$ violation is one of the necessary ingredients to describe the baryon asymmetry of the universe [6] and it is not clear yet, whether strength of $\mathcal{CP}$ violation as described by the SM is sufficient to explain the this observed asymmetry [7].

The note is organised as follows: the theoretical ansatz considered is explained in section 2. The MC samples and detector simulation are summarised in section 3, the selection of the $\mu^+\mu^-$ H final state in section 4. The method to determine the $\mathcal{CP}$ quantum numbers and to test $\mathcal{CP}$ invariance with emphasis on the formalism of the optimal observable is described in section 5. The results are discussed in section 6, and the note closes with a short conclusion in section 7.

2 Theoretical ansatz

We follow the ansatz of [8] for the parametrisation of the associated production of a scalar boson Φ with arbitrary $\mathcal{CP}$ properties with a vector boson Z.

In addition to the $\mathcal{CP}$ even SM like s-wave amplitude $\mathcal{M}_{\mathrm{H}Z}$ a new $\mathcal{CP}$ odd p-wave amplitude $\mathcal{M}_{\mathrm{A}Z}$ with coupling strength η contributes to the Higgs-strahlung process.

$$\mathcal{M}_{\phi Z} = \mathcal{M}_{HZ} + \eta \cdot \mathcal{M}_{AZ} \tag{1}$$

η is considered to be purely imaginary. In the SM η is zero, and in the MSSM a ZZA coupling is forbidden at Born level, but is induced via loop corrections. In general Two Higgs Doublet Models (2HDM) or other extensions of the Higgs sector η may be arbitrarily large.

The squared amplitude has three contributions:

$$|\mathcal{M}_{\Phi\mathrm{Z}}|^2 = |\mathcal{M}_{\mathrm{HZ}}|^2 + \eta \cdot 2Re(\mathcal{M}^*_{\mathrm{HZ}}\mathcal{M}_{\mathrm{AZ}}) + \eta^2|\mathcal{M}_{\mathrm{AZ}}|^2 \tag{2}$$

The first one reproduces the SM cross section. The second, linear in η, arises from the interference of the $\mathcal{CP}$ even and $\mathcal{CP}$ odd amplitudes is $\mathcal{CP}$ violating. The third is again $\mathcal{CP}$ conserving and increases the total cross section for the Higgs-strahlung process. The total cross section is given by [9]:

$$\sigma_{tot} = \frac{G_{\mathrm{F}}^2 M_{\mathrm{Z}}^6 \beta}{16\pi}\frac{1}{D_{\mathrm{Z}}(s)}(v_{\mathrm{e}}^2 + a_{\mathrm{e}}^2)(2 + \frac{s\beta^2}{6M_{\mathrm{Z}}^2} + \eta^2\frac{s^2\beta^2}{M_{\mathrm{Z}}^4}) \tag{3}$$

with $\beta = \sqrt{[s-(M_{\mathrm{Z}}+M_\Phi)^2][s-(M_{\mathrm{Z}}-M_\Phi)^2]}/s$, $D_Z(s) = (s - M_{\mathrm{Z}}^2)^2 + M_{\mathrm{Z}}^2\Gamma_{\mathrm{Z}}^2$, where $M_{\mathrm{Z}}, \Gamma_{\mathrm{Z}}$ denote the Z boson mass and width, G_{F} is the Fermi constant, v_{e} and a_{e} are the electron's vector and axial-vector couplings to the Z boson. The explicit analytic expression for the squared amplitude can be found in equations 2 and 3 of reference [8].

The $\mathcal{CP}$ properties can be analysed in a decay mode independent way by studying the angular distribution of the production θ_{Z} and of the decay of the Z into two fermions, described by two angles in the Z boson rest frame (ϕ^*, θ^*). The most sensitive variable is the production angle θ for which the differential cross section reads [9]:

$$\begin{aligned} \frac{\mathrm{d}\sigma}{\mathrm{d}\cos\theta} &= \frac{G_{\mathrm{F}}^2 M_{\mathrm{Z}}^6 \beta}{16\pi}\frac{1}{D_{\mathrm{Z}}(s)}(v_{\mathrm{e}}^2 + a_{\mathrm{e}}^2)\Big[1 + \frac{s\beta^2}{8M_{\mathrm{Z}}^2}\sin^2\theta \\ &+ \eta\frac{v_{\mathrm{e}}a_{\mathrm{e}}}{v_{\mathrm{e}}^2 + a_{\mathrm{e}}^2}\frac{2s\beta}{M_{\mathrm{Z}}^2}\cos\theta + \eta^2\frac{s^2\beta^2}{4M_Z^4}(1-\sin^2\theta/2)\Big] \end{aligned} \tag{4}$$

One finds that the term linear in η causes a $\mathcal{CP}$ violating forward backward asymmetry.

3 MC samples and detector simulation

All Monte Carlo samples have been generated with PYTHIA [10] including initial state radiation and the effect of beamstrahlung via the CIRCE program [11]. The response of the detector has been simulated with the fast simulation program SIMDET (Ver.3.01) [12]. The following background processes have been generated: $e^+e^- \to \mu^+\mu^-$, $e^+e^- \to W^+W^- \to \mu\mu\nu_\mu\nu_\mu$, $\tau\tau\nu_\tau\nu_\tau$ and $\mu\tau\nu_\mu\nu_\tau$, $e^+e^- \to ZZ \to$ all. Other background processes have been neglected. Given the results of the selection (see section 4) we consider the impact of this on our results to be small. The signal $e^+e^- \to ZH \to \mu^+\mu^-$ H has been generated for a Higgs boson mass of 120 GeV. The results are discussed for a centre-of-mass energy of 350 GeV and an expected integrated luminosity of 500 pb $^{-1}$.

4 Event selection

The branching ratios of the Higgs boson in the 2HDM or more exotic Higgs scenarios depend on several parameters and may differ quite largely from the values in the Standard Model [4]. In order not to limit the analysis to a particular Higgs model the aim is to perform an almost decay mode independent selection of $e^+e^- \to ZH \to \mu^+\mu^-$ H final state. Therefore only observables calculated from the muon momenta are used in the selection. In addition no explicit cut on the production angle of the di-muon system is applied, because this variable is the most sensitive variable for the determination of the $\mathcal{CP}$ properties of the Higgs boson.

The selection proceeds as follows:

1. At least two isolated muons are identified. The energy of the muon candidates has to exceed 15 GeV and they have to be isolated from all other charged particle tracks and energy depositions in the calorimeters by at least 10 degree. In case of more than two muon candidates found the pair with opposite charges being most consistent with decay of the Z boson is used in the following steps of the selection.

2. The invariant mass of the two muons has to be consistent with the Z boson hypothesis within 5 GeV: $|M_{\mu^+\mu^+} - M_Z| < 5$ GeV. This removes large parts of the WW background and $Z/\gamma \to \mu^+\mu^-$ events without hard photon radiation in the final state.

3. The recoil mass to the di-muon system has to be consistent with the H boson hypothesis within 5 GeV: $|M_{\mathrm{recoil}} - M_{\mathrm{H}}| < 5$ GeV. This removes large parts of the ZZ background and Z/$\gamma \rightarrow \mu^+\mu^-$ events with hard photon radiation in the final state.

4. Finally the absolute z-component of the di-muon momentum should be smaller than 120 GeV. This removes a significant part of the remaining background from the ZZ and Z/$\gamma \rightarrow \mu^+\mu^-$ events with hard photon radiation in the final state.

The distribution of the variables used in cuts (2) to (4) is shown in figure 1.

The performance of the selection is summarized in table 1. After the final cut 473 background events remain dominated by the contribution from Z pair production. The efficieny for the signal process is 37.7 % assuming SM branching ratios and angular distributions. This corresponds to 981 events and a signal-to-background ration of better than 2/1. The efficiencies

Cut	Total BG	$\mu^+\mu^-$	W^+W^-	ZZ	Eff. %	$N_{\mathrm{H}Z}$
1	591663	499873	56860	34930	81.8	2128
2	263252	243700	1799	17753	66.1	1700
3	3340	2502	26	812	40.1	1042
4	473	55	18	400	37.7	981

Table 1: *Number of remaining background events, signal efficiency and number of expected signal events after each of the four cuts.*

for several individual decay modes of the Higgs boson are shown in fig. 2 (left). The signal efficiencies vary by 4% absolute. The $\cos\theta$ distribution of the selected events is shown in in fig. 2 (right). Due to decreasing muon identification performance and the cut on the z-component of the di-muon momentum the efficiency for $\cos\theta > 0.9$ is close to zero.

5 Methodology

The most sensitive kinematic variable for the determination of η is the production angle $\cos\theta$. It is straightforward to perform a binned maximum likelihood fit to its distribution. The reference distributions for arbitrary

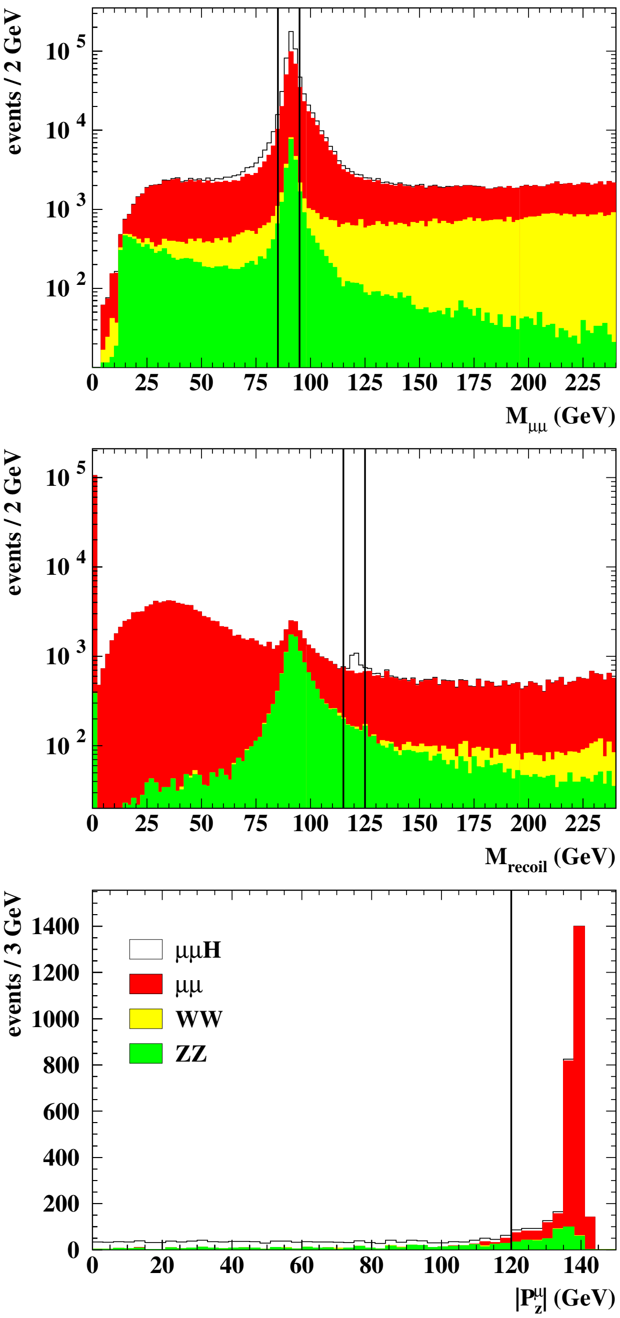

Figure 1: *Distribution of variables used in the selection. The vertical lines indicate the position of the cuts. Open histogram: HZ signal, black $Z/\gamma \rightarrow \mu^+\mu^-$, light gray WW and dark gray ZZ background.*

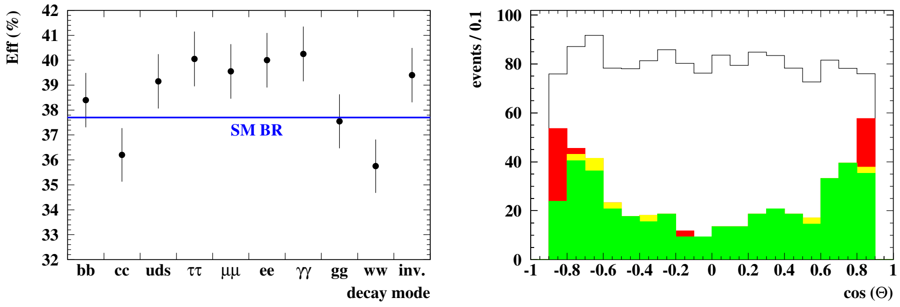

Figure 2: *Selection efficiencies for various Higgs decay modes (left) (the line indicates the efficiency assuming SM branching ratios) and* $\cos\theta$ *distribution of the selected events (right). Open histogram HZ signal, black* $Z/\gamma \to \mu^+\mu^-$*, light gray WW and dark gray ZZ background.*

values of η are obtained from the one for $\eta = 0$ by reweighting each event according to the threefold differential cross section in θ, θ^*, ϕ^*, i.e. the weight w is given by $w = \frac{|\mathcal{M}_{Z\Phi}(\eta)|^2}{|\mathcal{M}_{Z\Phi}(\eta=0)|^2}$. Distributions of the production angle for different values of η are shown in fig. 3.

The reliability of the reweighting method has been checked by generating the angular distributions for pure $\mathcal{CP}$ odd ZZA coupling from an event sample with SM like ZZH coupling and comparing them to the analytic expression. No deviation from the predicted shape has been observed.

However the sensitivity can be increased by including the decay angles of the muon in the Z rest frame, which also carry information about the $\mathcal{CP}$ quantum numbers of the Higgs boson. In principle a maximum likelihood fit to the three dimensional distribution allows to determine η with the highest accuracy possible. But this technique requires a huge amount of MC events in order to obtain reliable and stable results. This problem can be circumvented by using the formalism of the optimal observable.

5.1 Optimal observable

The method of optimal observables [13–16] has been proposed for the estimation of coupling parameters if the differential cross section is of the form $\mathrm{d}\sigma/\mathrm{d}\Omega = \mathrm{d}\sigma_{\mathrm{SM}}/\mathrm{d}\Omega + \eta \mathrm{d}\sigma_{\mathrm{new}}/\mathrm{d}\Omega$. The optimal observable for this kind of problem is given by the ratio of the new contribution to the cross section

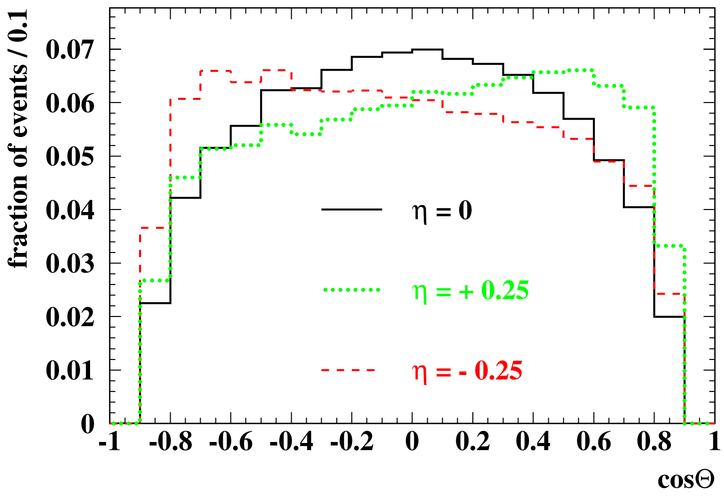

Figure 3: *cosθ-distributions for different values of η (normalised to unity). η = 0 solid, η = + 0.25 dotted and η = + 0.25 dashed.*

over the SM contribution. For each event this optimal observable is calculated from the kinematics. It has been proven [14] that a maximum likelihood fit to the distribution of the optimal observable has exactly the same sensitivity as a maximum likelihood fit to the manyfold cross section, which means that the whole information about η is combined in this single observable. The formalism has so far been used experimentally in the measurement of the τ polarisation [17], the determination of the weak dipole moment of the τ lepton [18], and the measurement of the Tripe Gauge Couplings [19].

For our problem the optimal observable $\mathcal{O}$ is given by

$$\mathcal{O} \equiv \frac{\sigma_{\mathcal{CP}}}{\sigma_{\mathrm{SM}}} \equiv \frac{2Re(\mathcal{M}^{*}_{ZA}\mathcal{M}_{\mathrm{ZA}})}{|\mathcal{M}_{\mathrm{ZH}}|^2} \tag{5}$$

neglecting the contribution quadratic in η. The choice of the observable is very close to optimal for small η. But even for larger η the maximum sensitivity can be recovered in several ways as pointed out in [20, 21]. Distributions of the optimal observable for different values of η are shown in fig. 4.

Another simplification in the extraction of η can be achieved by considering only the mean value of the optimal observable $< \mathcal{O} >$. It has been

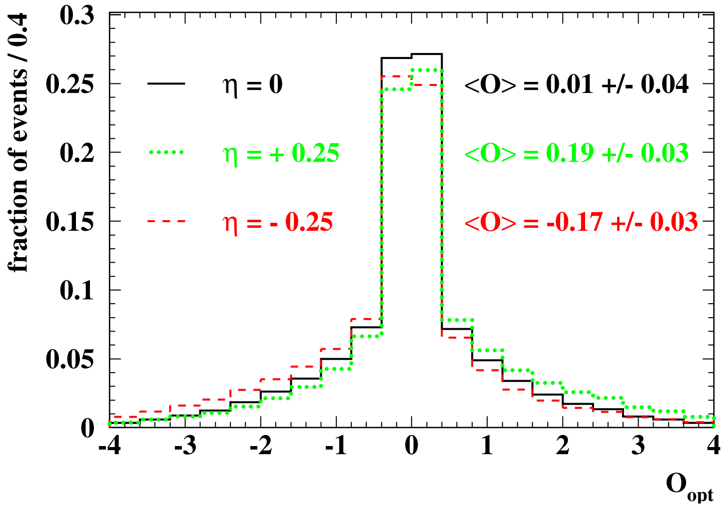

Figure 4: *Distributions of the optimal observable for different values of* η *(normalized to unity) (left), and the asymmetry caused by the CP violating contribution (right):* η *= 0 solid,* η *= + 0.25 dotted and* η *= + 0.25 dashed*

shown [14] that for modest values of η almost all the information about η is contained in the first moment of the distribution of $\mathcal{O}$. After this restriction the extraction of η is very simple. The value of η can be read from a 'gauge' curve including confidence belt (see light shaded area in fig. 5), where the expected mean value of the optimal observable is shown depending on the magnitude of η: E($< \mathcal{O} >$)(η). The maximum sensitivity (steepness of the gauge curve) is obtained for values of η close to zero. For larger values the sensitivity is decreased due to influence of the η^2 contribution to the cross section, which has been neglected in the construction of the optimal observable. This loss is compensated by taking into account the dependence of the total cross section on η (dark shaded area in fig. 5). The steepness of this second gauge curve is complementary to the behaviour of the gauge curve for $< \mathcal{O} >$. Technically η is determined by minimising the following χ^2:

$$\chi^2(\eta) = \frac{[< \mathcal{O} >_{meas.} - E(< \mathcal{O} >)(\eta)]^2}{\sigma_{exp.}(\eta)} + \frac{[N_{meas.} - N_{exp}(\eta)]^2}{N_{exp}(\eta)}. \qquad (6)$$

The first term corresponds to the gauge curve for the the mean value of the optimal observable and the second to the one for the total cross section.

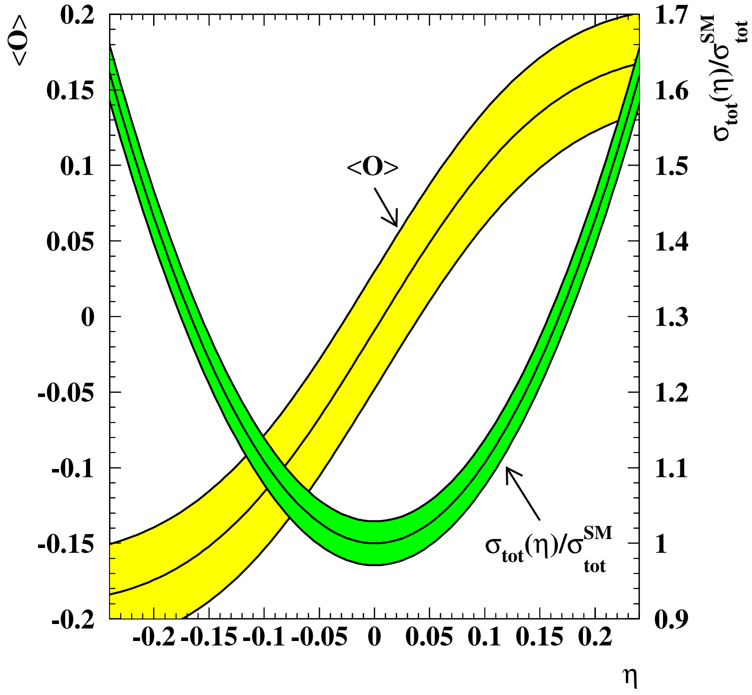

Figure 5: *Gauge curves for the estimation of η: light shaded area for the mean value of the optimal observable, dark shaded area for the measurement of the total cross section. The band correspond to the expected 1σ error contours.*

5.2 Test of $\mathcal{CP}$ invariance

The optimal observable in equation 5 is $\mathcal{CP}$ odd. If the Higgs-strahlung process respects $\mathcal{CP}$ symmetry the expectation value of the optimal observable must vanish, i.e. $<\mathcal{O}>=0$. Any significant observed deviation from zero implies the existence of $\mathcal{CP}$ violation. This conclusion does not depend on the theoretical ansatz of equation 1, but is a completely model independent test of $\mathcal{CP}$ invariance. However for the form of the lagrangian assumed this $\mathcal{CP}$ odd optimal observable is the most effective of all possible $\mathcal{CP}$ odd observables in the detection of $\mathcal{CP}$ violation [22].

5.3 Comparison of methods

The three methods for extracting η (1) maximum likelihood fit to the $\cos\theta$ distribution, (2) maximum likelihood fit to the optimal observable distribution and (3) using the mean value of the optimal observable have been compared with respect to the their sensitivity. The study has been performed with and without taking into account the dependence of the total cross section on η. As an example the $2 \times \Delta$ log-likelihood, $\Delta\chi^2$ curves, respectively, for 3 three methods are compared in fig.6.

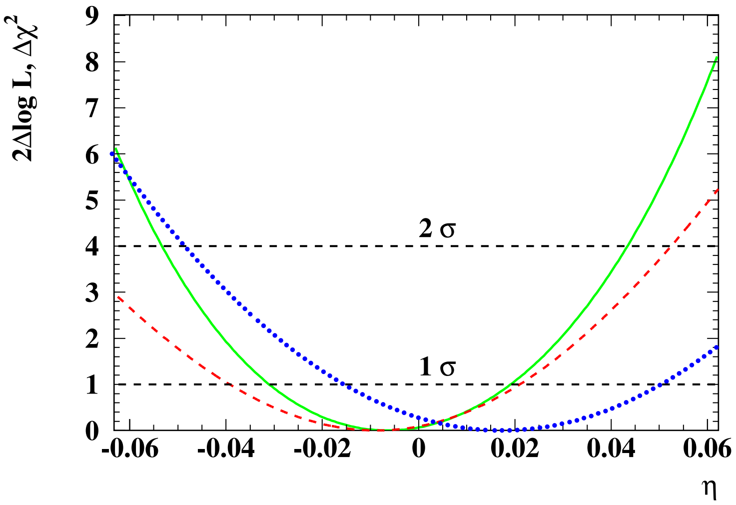

Figure 6: $2 \times \Delta$*log-likelihood,* $\Delta\chi^2$ *curves for three different methods of extracting* η*: (1) cos*θ *distribution (dotted), (2) mean value of optimal observable (dashed) and (3) mean value of optimal observable and total cross section (dotted).*

The results of the comparison are summarised in table 2 for signal events after the selection. The numbers quoted are average values from 80 samples each corresponding to a recorded luminosity of 500 pb^{-1}. The use of the optimal observable improves the sensitivity significantly compared to using $\cos\theta$ only. The use of the mean value of the optimal observable instead of performing a maximum likelihood fit to the distribution of $\mathcal{O}$ does not decrease the accuracy in the determination of η. For the further studies including the remaining background only the extraction of η with the mean value of the optimal observable is considered.

method	w/o σ_{tot}	with σ_{tot}
	$\Delta\eta$	
$\cos\theta$	0.046	0.033
$opt.obs.\mathcal{O}$	0.032	0.026
$< \mathcal{O} >$	0.032	0.026

Table 2: *Comparison of sensitivity of methods.*

6 Results

The gauge curves taking into account the loss in sensitivity due to the remaining background are shown in figure 7. The value of η can be determined with an accuracy of $\Delta\eta = 0.038$ using the mean of the optimal observable only and of $\Delta\eta = 0.032$ when adding the information from the measurement of the total cross section. Comparing this to the numbers obtained neglecting the background contamination we find that the accuracy is decreased by 0.006 or 20% relative. The errors quoted are again the average values from 80 samples each corresponding to a recorded luminosity of 500 pb^{-1}. The estimation of the accuracy has been checked by studying the confidence interval coverage, i.e. the percentage of cases in which the true value falls in the 1σ (2σ) confidence intervals has been determined. In the limit of large numbers of trials the coverage should be 68.3% (95.5%) for the 1σ (2σ) confidence intervals. Using the mean values of the optimal observable only the coverage reads 75.0±5.0% (93.8±2.5%) for 1σ (2σ) and adding the information from the total cross section 71.3±5.0% (95.0±2.5%) for 1σ (2σ). From this we conclude that the estimate of the statistical error is reliable.

7 Conclusion

A future e^+e^- linear collider will allow to determine the $\mathcal{CP}$ properties of Higgs bosons with high accuracy by analysing the angular distributions of the final state fermions in the Higgs-strahlung process. The use of an $\mathcal{CP}$ odd optimal observable maximises the sensitivity for the determination of η and provides a true test of $\mathcal{CP}$ invariance independent of the theoretical ansatz chosen. The accuracy in the determination of η taking into account the selection efficiency, detector resolution and background contamination is

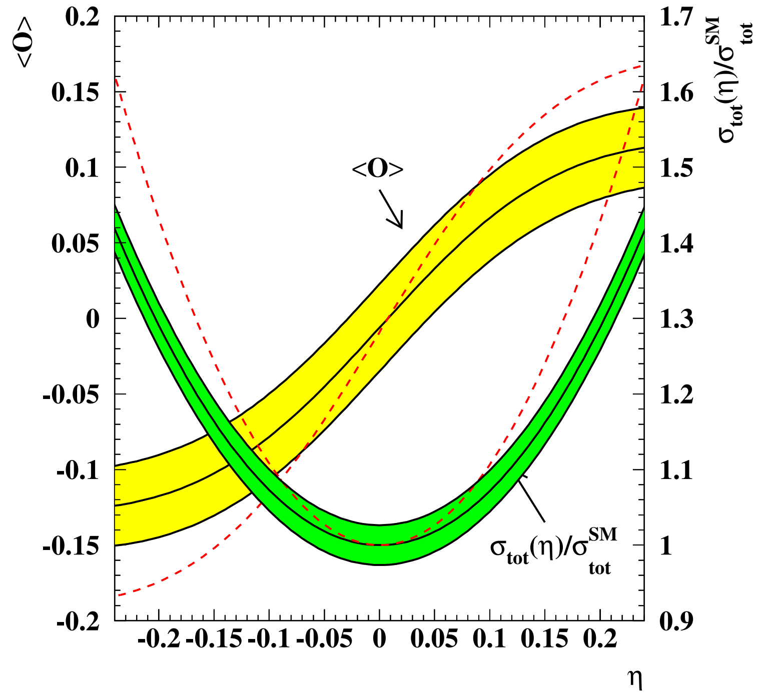

Figure 7: *Gauge curves including the effect of the background contamination for the estimation of η: light shaded area for the mean value of the optimal observable, dark shaded area for the measurement of the total cross section. The band correspond to the expected 1σ error contours. The dashed lines show the 'gauge' curves neglecting the remaining background.*

0.032 using the mean value of the observable and the information from the total cross section, and 0.038 neglecting the latter one using only $Z \to \mu\mu$ decays. Further increases in sensitivity can be obtained from the inclusion of the Z$\to$ e^+e^- decay.

8 Acknowledgements

Numerous helpful discussions with B. Kniehl, K. Desch and P. Zerwas are greatfully acknowledged.

References

[1] P. W. Higgs, Phys. Lett. **12** (1964) 132; Phys. Rev. Lett. **13** (1964) 508;
F. Englert und R. Brout, Phys. Rev. Lett. **13** (1964) 321;
G. S. Guralink, C. R. Hagen und T. W. B. Kibble, Phys. Rev. Lett. **13** (1964) 585;
P. W. Higgs, Phys. Rev. **155** (1966) 1156;
T. W. B. Kibble, Phys. Rev. **155** (1967) 1554.

[2] S. Weinberg, Phys. Rev. Lett. **19** (1967) 1264;
A. Salam, *Elementary Particle Theory,* ed. N. Svartholm (Almquist und Wiksells, Stockholm, 1968), 367;
D. L. Glashow, J. Iliopoulos und L. Maiani, Phys. Rev. **D2** (1970) 1285;
S. Weinberg, Phys. Rev. **D5** (1972) 1412.

[3] H.P. Nilles, Phys. Rep. **110** (1984) 1;
H.E. Haber and G.L. Kane, Phys. Rep. **117** (1985) 75;
R. Barbieri *et al.*, *Z Physics at LEP1*, CERN 89-08, Vol. 2, 121;
J.M. Frère and G.L. Kane, Nucl. Phys. **B223** (1983) 331;
J. Ellis *et al.*, Phys. Lett. **B123** (1983) 436;
J. Ellis *et al.*, Phys. Lett. **B127** (1983) 233.

[4] J. F. Gunion, H. E. Haber, G. L. Kane und S. Dawson, *The Higgs Hunter's Guide*, (Addision-Wesley Publishing Company, Reading, MA, 1990).

[5] V. Barger *et al.*, Phys. Rev. **D49** (1994) 79;
K. Hagiwara *et al.*, Z. Phys. **C62** (1994) 99;
K. Hagiwara *et al.*, Eur. Phys. J. **C14** (2000) 457.

[6] A. D. Sakharov, *JETP Lett.* **5**, 24 (1967).

[7] G. R. Farra and M. E. Shaposhnikov Phys. Rev. Lett. **70** (1993) 2833, (E): **72** (1993) 210 *and* Phys. Rev. **D50** (1994) 774;
M. B. Gavela, Nucl. Phys. **B430** (1994) 345;
P. Huet and E. Sather, Phys. Rev. **D51** (1995) 279.

[8] A. Djouadi , B. A. Kniehl, DESY 93-123C, page 51.

[9] B. A. Kniehl, private communication.

[10] T. Sjostrand, Comp. Phys. Comm. **82** (1994) 74.

[11] T. Ohl, Comp. Phys. Comm. **101** (1997) 296

[12] M. Pohl and H. J. Schreiber, "SIMDET - Version 3: A parametric Monte Carlo for a TESLA detector," DESY-99-030.

[13] D. Atwood, A. Soni, Phys. Rev. **D45** (1992) 2405.

[14] M. Davier, L. Duflot, F. Le Diberder, A. Rougé Phys. Lett. **B306** (1993) 411.

[15] J. Gunion *et al.*, Phys. Rev. Lett. **77** (1996) 5172.

[16] M. Diehl, O. Nachtmann, Z. Phys. **C62** (1994) 397

[17] ALEPH Collaboration, D. Buskulic *et al.*, Z. Phys. **C69** (1996) 183

[18] OPAL Collaboration, K. Ackerstaff *et al.*, Z. Phys. **C74** (1997) 403; OPAL Collaboration, R. Akers *et al.*, Z. Phys. **C66** (1995) 31.

[19] OPAL Collaboration,G. Abbiendi *et al.*, CERN-EP-2000-114; DELPHI Collaboration, P. Abreu *et al.*, Phys. Lett. **B459** (1999) 382; ALEPH Collaboration, R. Barate *et al.*, Phys. Lett. **B422** (1998) 369.

[20] H. Voss, *PhD thesis*, BONN-IR-2000-04.

[21] M. Diehl, O. Nachtmann, Eur. Phys. J. **C1** (1998) 177.

[22] P. Overmann, *PhD thesis*, Heidelberg, HD-THEP-92-38.